Colloid Polym Sci 277:436–445 (1999)

ORIGINAL CONTRIBUTION

A. Dahlberg
A. Larsson
B. Åkerman
S. Wall

2-(*p*-toluidino)-6-naphthalene sulfonate as a fluorescent probe for flocculation studies of cationic potato amylopectin and nanosized silica particles. 2. Flocculation by binding of nanosized silica particles

Received: 14 August 1998
Accepted in revised form: 4 December 1998

A. Dahlberg · A. Larsson (✉) · S. Wall
Department of Physical Chemistry
Göteborg University, Kemigården 3
S-412 96 Göteborg, Sweden
e-mail: zoombie@phc.chalmers.se
Tel.: +46-31-7722748
Fax: +46-31-167194

B. Åkerman
Department of Physical Chemistry
Chalmers University of Technology
Kemigården 3, S-412 96 Göteborg, Sweden

Abstract 2-(*p*-toluidino)-6-naphthalene sulfonate (TNS) is a probe that fluoresces strongly when bound to certain proteins and polymers, but weakly in aqueous solutions. The reversible association of TNS is used to monitor the binding of anionic nanosized silica particles (NSP) to cationic potato amylopectin starch (CApS) through the decreasing fluorescence emission as TNS is competitively released by the particle binding. Steady-state fluorescence measurements at different mixing ratios of CApS and NSP provide data on the equilibrium binding. The isotherm derived is used to establish the fact that the most efficient flocculation between CApS and NSP occurs when the polymer coils are nearly saturated by NSP, but still have positively charged parts left. This supports a patch-flocculation mechanism. Stopped-flow experiments show that NSP binding to CApS occurs within a few milli seconds. This observation allows turbidity changes which occur on longer timescales to be ascribed to particle-decorated polymers undergoing changes in the conformation or aggregation.

Key words Retention aids – Flocculation – Fluorescence – 2-(*p*-toluidino)-6-naphthalene sulfonate – Starch – Silica

Introduction

In the first part of this report [1] it was shown how the fluorescent probe 2-(*p*-toluidino)-6-naphthalene sulfonate (TNS) binds to cationic amylopectin potato starch (CApS) at a single type of binding site. The binding is due to an electrostatic component superimposed on a nonelectrostatic contribution at least partly caused by hydrogen bonding. A useful feature is that the fluorescence emission of TNS is much stronger when bound to CApS than in water, so the emission intensity can be used to monitor the amount of bound TNS. At 5 mM NaCl the affinity is approximately equally shared between the electrostatic and nonelectrostatic contributions, and the association constant is low, $110 \pm 20\ M^{-1}$. In the present paper, the TNS emission intensity is used to monitor the association between anionic naznosized silica particles (NSP) and CApS, through the competitive release of the weakly bound TNS. Comparison is also made with the related effect of TNS release by added salt, which was studied in the first paper. Both equilibrium and kinetic aspects of particle binding to CApS at 5 mM NaCl are addressed. This provides valuable information for the interpretation of earlier stopped-flow studies [2] of the kinetics of flocculation of NSP by CApS under similar conditions, performed with turbidity detection. The main idea is that TNS release reflects the actual particle binding, whereas turbidity also reflects changes in polymer conformation.

Materials and methods

Materials

The NSP were donated by Eka Chemicals AB (Bohus, Sweden) and were used as received. The other components and their preparation is discussed in Ref. [1].

The silica particles

The NSP have a spherical radius of 7 nm as measured by static light scattering and a hydrodynamic radius of 9.5 nm as measured by dynamic light scattering [3]. This make them considerably smaller than the radius of gyration of the amylopectin coils [4]. The particles have a surface area of about 500 m^2/g (as given by the manufacturer) and have roughly the shape of a prolate ellipsoid [5].

The silanol group dissociates in water

$$SiOH = SiO^- + H^+$$

meaning that the surface charge is strongly pH dependent. All investigations were performed at pH = 8, and since the point of zero charge is about 2 [6] the particles are negatively charged at the pH used. The NSP (stock solution 15.2%wt) were diluted with water, and the pH was adjusted to 8.0 with a few drops of dilute HCl(aq) or NaOH(aq). The solution was degassed for 30 min, in order to avoid bubble formation in the stopped-flow experiments.

Instruments

Steady-state fluorescence spectra were recorded on a SPEX fluorolog τ2. Stopped-flow experiments were performed with either fluorescence (Bio-Logic, 425 nm longpass filter) or turbidity detection (Hi-Tech Scientific). The excitation wavelength was 315 nm unless stated otherwise. No corrections for inner-filter effects were made. If not otherwise stated the measurements were performed in 5 mM NaCl at pH 8 and at room temperature.

When spectra were recorded at mixing ratios of CApS and NSP close to 1:1, opaque flocs caused large fluctuations in the absorption if the flocculation was allowed to proceed unhindered. The larger flocs were therefore resuspended into smaller units of manageable size by mixing.

Results

Steady-state measurements

Emission spectra of TNS in the presence of a constant concentration of CApS and a varying concentrations of added NSP are shown in Fig. 1. The spectra were recorded 15 min after mixing and correspond to the equilibrium conditions (except in the white floc region where mixing was performed). The spectra were normalized at 375 nm in order to correct for light scattering from the polyelectrolyte complexes formed. It is seen that in the absence of NSP (top curve) TNS binds to the CApS sites with an emission maximum at 460 nm, as reported earlier. Importantly, addition of NSP leads to

Fig. 1 Emission spectra of 2-(*p*-toluidino)-6-naphthalene sulfonate (*TNS*) in cationic amylopectin starch (CApS) solution with various concentrations of added nanosized silica particles (*NSP*). The excitation wavelength was 315 nm. The weight concentration of TNS was 0.0005% and the weight concentration of CApS was 0.05%. The concentrations of NSP are given in weight percent. The NaCl concentration was 5 mM and the pH was 8.0. The spectra were normalised at 375 nm to the same intensity in order to allow for light scattering from the polyelectrolyte complexes formed

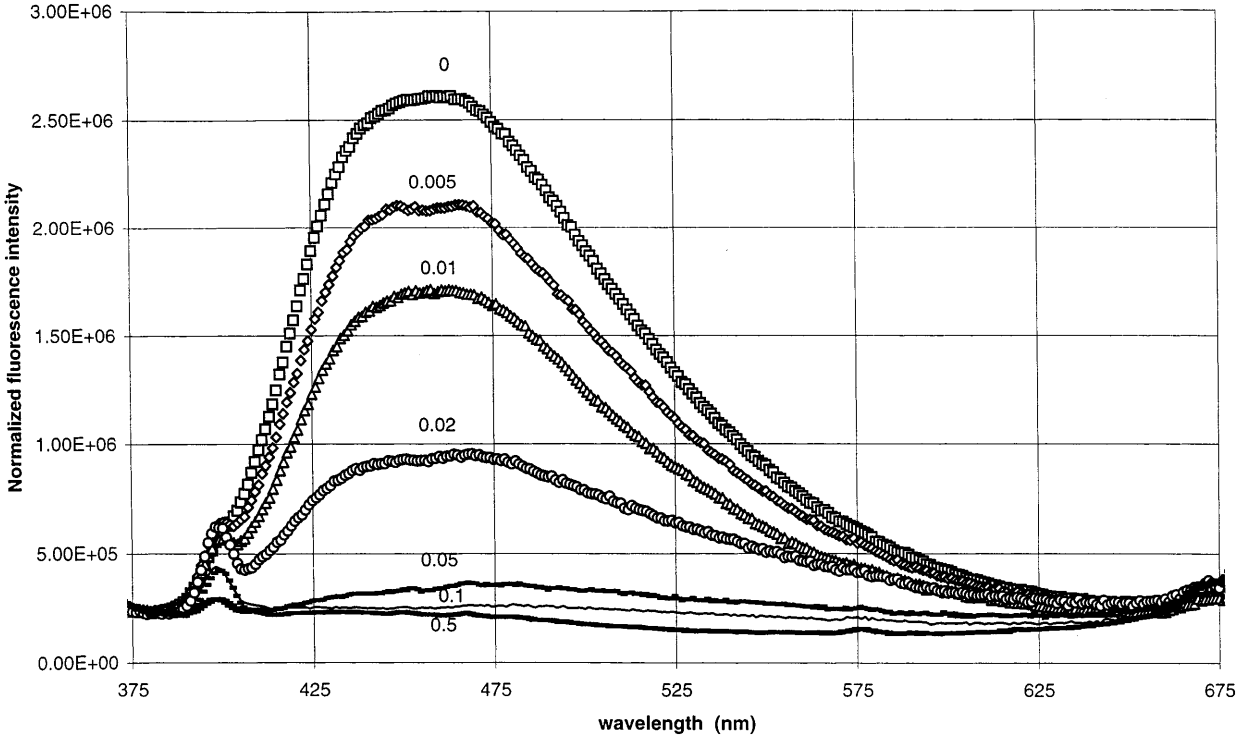

a progressively decreasing emission intensity, but the spectral shape is essentially retained.

The fluorescence intensity at the 460 nm maximum as a function of the added NSP concentration is shown in Fig. 2a. The intensity is seen first to decrease, and then to plateau for NSP concentrations above 0.1%. The final intensity level corresponds to about 4% of the initial intensity (no NSP). This is similar to the intensity observed for TNS in water, and is much lower than the 50% remaining intensity for TNS bound to CApS at high salt, i.e. nonelectrostatically [1].

The silica particles themselves did not show any fluorescence in the wavelength range examined. Furthermore, when TNS was mixed with NSP (without CApS present) the resulting emission spectra were identical to that measured for TNS fluorescence in water (results not shown). Hence, TNS does not bind to NSP, as expected since both components are negatively charged.

The effect on the TNS emission when the silica particles were added to a native amylopectin potato starch (NApS)-TNS solution is shown in Fig. 3. Using the same intensity scale as in Fig. 1 for the sake of comparision, in the range 0–0.1% where the emission with CApS gradually decreases to zero there is only a small decrease in TNS emission with NApS.

Kinetic measurements

For the TNS approach to be useful in flocculation investigations, it was important to establish to what extent the TNS probe perturbs the process under study. The flocculation kinetics of CApS and NSP with and without TNS present was therefore followed in stopped flow, using as a detection method turbidimetry at 660 nm where TNS does not absorb [1]. The turbidity traces with and without TNS at two different mixing ratios are compared in Fig. 4a. The shapes of the curves are not affected, and the differences in amplitude are within the experimental variation between different experiments in the absence of TNS [2]. We conclude that TNS may affect the size of the flocs, but not the principal mechanism of their formation. In particular a maximum in turbidity is observed at a mixing ratio of $m_{NSP}/m_{CApS} = 5$, whereas no such maximum occurs at a mixing ratio of $m_{NSP}/\ m_{CApS} = 1$, in agreement with earlier observations [2]. In order to better understand the mechanism underlying these different types of behavior we therefore turned to fluorescence-detected stopped-flow measurements.

The fluorescence intensities as a function of time for the mixing of 0.01%wt CApS with solutions of different NSP concentrations are shown in Fig. 5. The case with no added NSP coincides with the result shown in Fig. 4b (which will be discussed later) even though the mixing in this case was exactly the same as when NSP was added. All solutions used for mixing contained 0.005%wt TNS and 5 mM NaCl in order to maintain these concentrations throughout the mixing. When no NSP is added the response stays essentially constant at about roughly 8 V. When NSP is added the traces start at considerably lower levels (1–2 V) than with no NSP, and the more so the higher the NSP concentration. This shows that there is a large decrease in the fluorescence intensity which is faster than the time resolution of the instrument (1 ms). After this fast process, which will be intrepreted as release of TNS from CApS, a slow and weak growth of the fluorescence over many seconds follows.

Turbidity-detected measurements showed that at the low concentrations of NSP and CApS used in the fluorescence measurements there was no detectable turbidity at 315, 440, 460 and 480 nm. Fluorescence-detected control experiments, in the absence of NSP, showed that upon mixing CApS with TNS there is an increase in TNS emission (compared to the level observed if CApS is mixed with a solution without TNS) which again occurs faster than the 1 ms time resolution, indicating very fast association of TNS to CApS. Similarly dilution of a CApS-TNS solution with 5 mM NaCl(aq) (with no TNS) gave a decrease in initial intensity (Fig. 4b) but was thereafter constant in the time range of the stopped flow. This shows that the salt-induced dissociation of CApS-bound TNS also occurs faster than 1 ms.

Discussion

Phase diagram

The flocculation behavior between CApS and NSP has previously been reported in terms of a phase diagram (Ref. [2], Fig. 6). This characterization was performed in the absence of TNS, and an important question is whether the TNS probe affects the flocculation behavior. We have not remeasured the phase diagram in the presence of TNS, but turbidity-detected stopped-flow studies with and without TNS (Fig. 4a) showed that the effect of TNS was small. Only a small perturbation by TNS is expected since the amount of TNS probe initially bound to CApS is very low under the present conditions. The molar ratio of bound TNS to the total glucose monomer concentration was estimated to be 1.6×10^{-3} (see Appendix). With 4% of the monomers being cationized this means that 1 out of 25 cationic sites are occupied by TNS. Secondly, these few bound TNS molecules are not likely to affect the kinetics of particle binding, since control experiments showed that TNS dissociates on timescales faster than 1 ms (Fig. 4b). This is consistent with what we observed for the two types of turbidity curves at certain mixing ratios of NSP and CApS reported earlier [2] also in the presence of TNS.

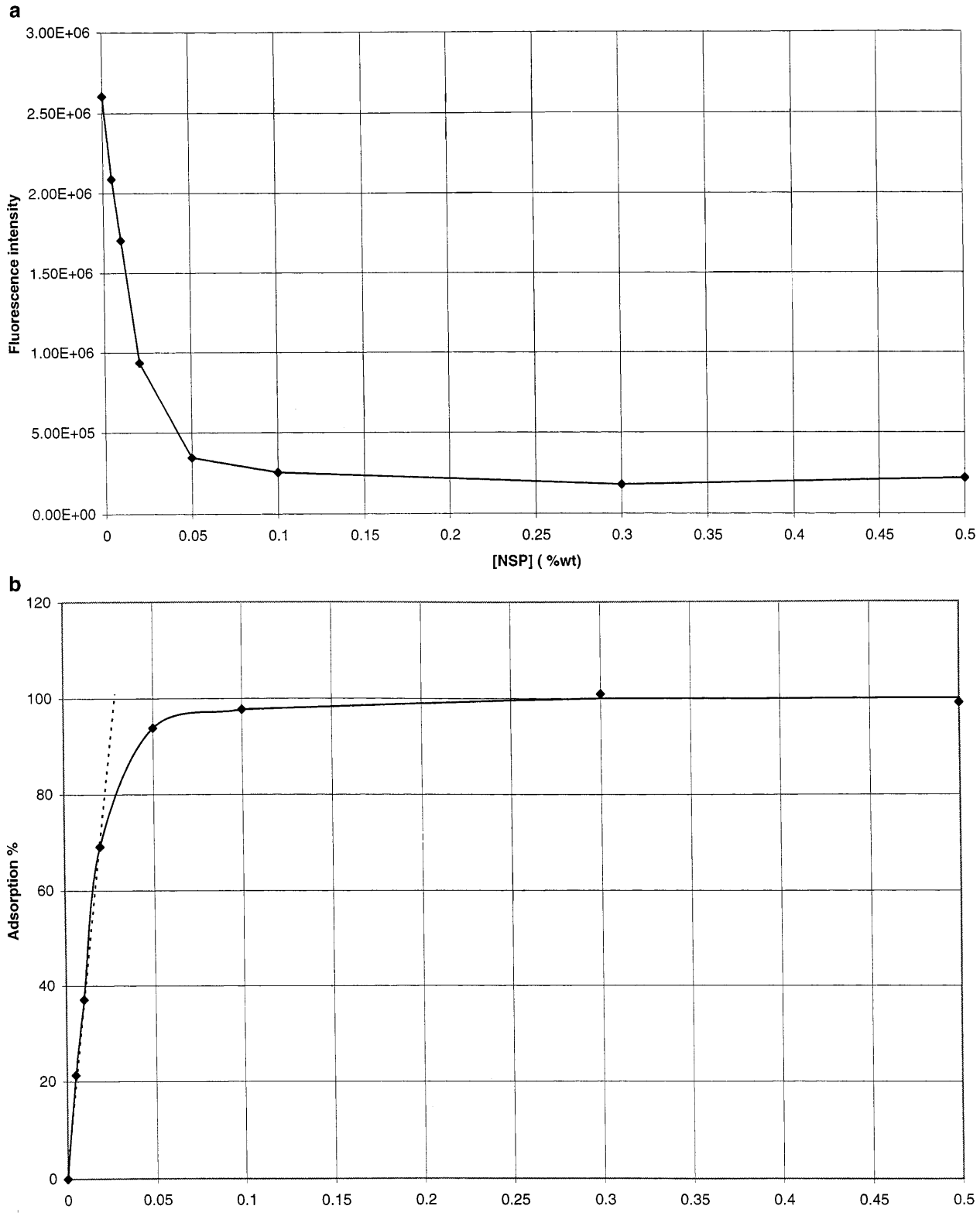

Fig. 2 a The fluorescence intensity at 460 nm emission as a function of NSP concentration. The experimental conditions as in Fig. 1. **b** The number of available cationic sites occupied by NSP. The experimental conditions as in Fig. 1

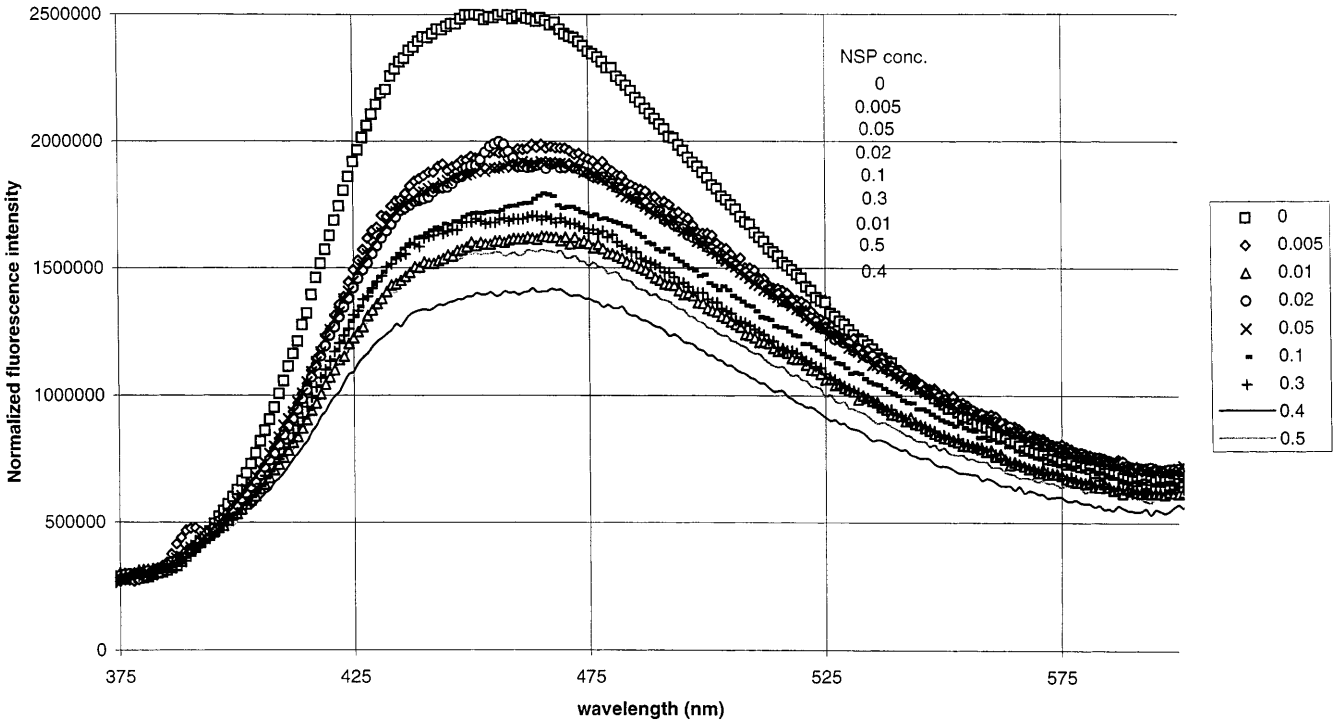

Fig. 3 Emission spectra of TNS in native amylopectin starch solution with various concentrations of added NSP. The excitation wavelength was 315 nm. The weight concentration of TNS was 0.0005% and the weight concentration of amylopectin was 0.05%. The concentrations of NSP are given in weight percent. The NaCl concentration was 5 mM and the pH was 8.0. The notation *NSP conc.* denotes the order in which the data appear at 460 nm

We will therefore use the phase diagram in the absence of TNS (Fig. 6) as a basis for the discussion of the underlying mechanisms of the two flocculation types.

In the black areas of Fig. 6 transparent flocs are formed and in the grey area there are white flocs. In the white area there are no visible flocs. In the case of dilute starch solutions (concentration below the overlap concentration of $c^* = 4$ mg/ml) it was found that white flocs only formed in a narrow regime centered at the line corresponding to a 1:1 (weight:weight) mixing ratio of CApS and NSP; otherwise transparent flocs were formed unless the excess of NSP was too large (white area). Laser diffractometry showed that in the dilute CApS regime ($c_{\mathrm{CApS}} < c^*$) the white flocs had a typical radius of 60 μm [2], and thus contained a large number of CApS-NSP complexes, while the transparent flocs contained only a few. Above c^* only white flocs were observed. Here focus has been on the dilute regime, an approach which is facilitated by the fluorescence detection since it is more sensitive than turbidity.

Steady-state measurements

Since the NSP do not bind TNS themselves, the decreases in TNS emission upon addition of NSP (Fig. 1) must reflect the release of TNS by competitive binding by NSP to CApS. This is the basis for our use of TNS as a probe for NSP binding. Furthermore, we conclude that the particles primarily bind to cationic sites on CApS. Since there is a very small decrease in emission, i.e. much less release of TNS when the same particles are added to NApS which lack cationic sites (Fig. 3).

The comparison between CApS and NApS can be taken one step further, however. The almost absence of TNS release in the NApS case shows that the NSP do not compete substantially with the nonelectrostatic interaction which binds TNS to NApS [1]. This nonelectrostatic component is also present in binding to CApS [1], and represents a considerable 50% of the affinity of TNS for CApS at the 5 mM ionic strength used [1]. It is therefore interesting to note that all TNS molecules can be displaced from CApS if enough particles are added, as can be concluded from the observation that in Fig. 1 the emission intensity level reaches that of TNS in water at high enough NSP concentration. (This is about 3% of the intensity observed without NSP in Fig. 2 [1].) Since the NApS results show that NSP cannot compete fully with the nonelectrostatic binding component of TNS, complete TNS displacement from CApS is possible only if the

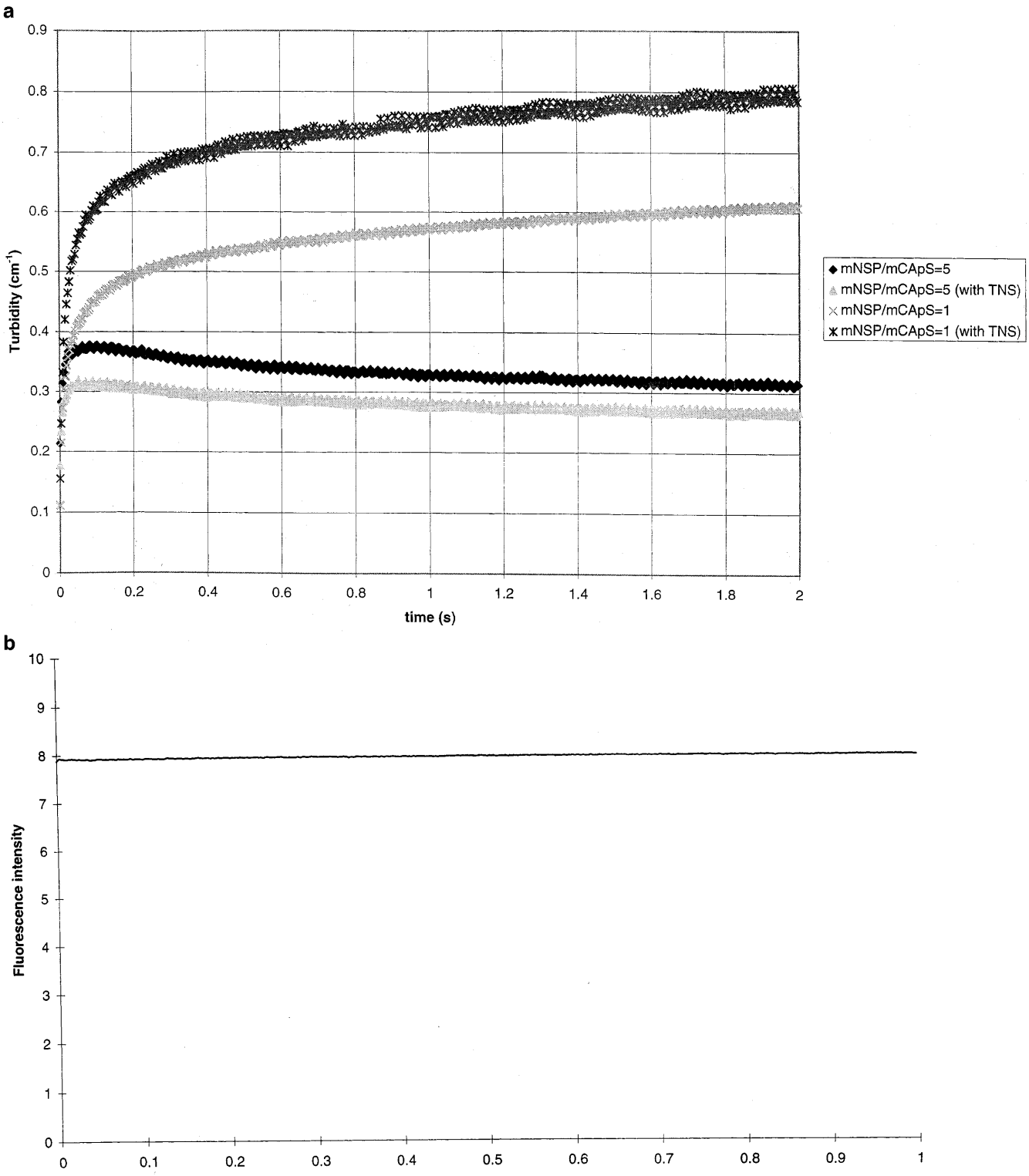

Fig. 4 a Stopped-flow turbidity traces of mixing of CApS (0.1%wt) and NSP (0.1 or 0.5%wt) in the absence or presence of (0.05%wt) TNS. 5 mM NaCl, pH 8.0. **b** Dissociation kinetics of the TNS-CApS complex measured by TNS fluorescence after mixing the complex with a solution of 5 mM NaCl, pH 8

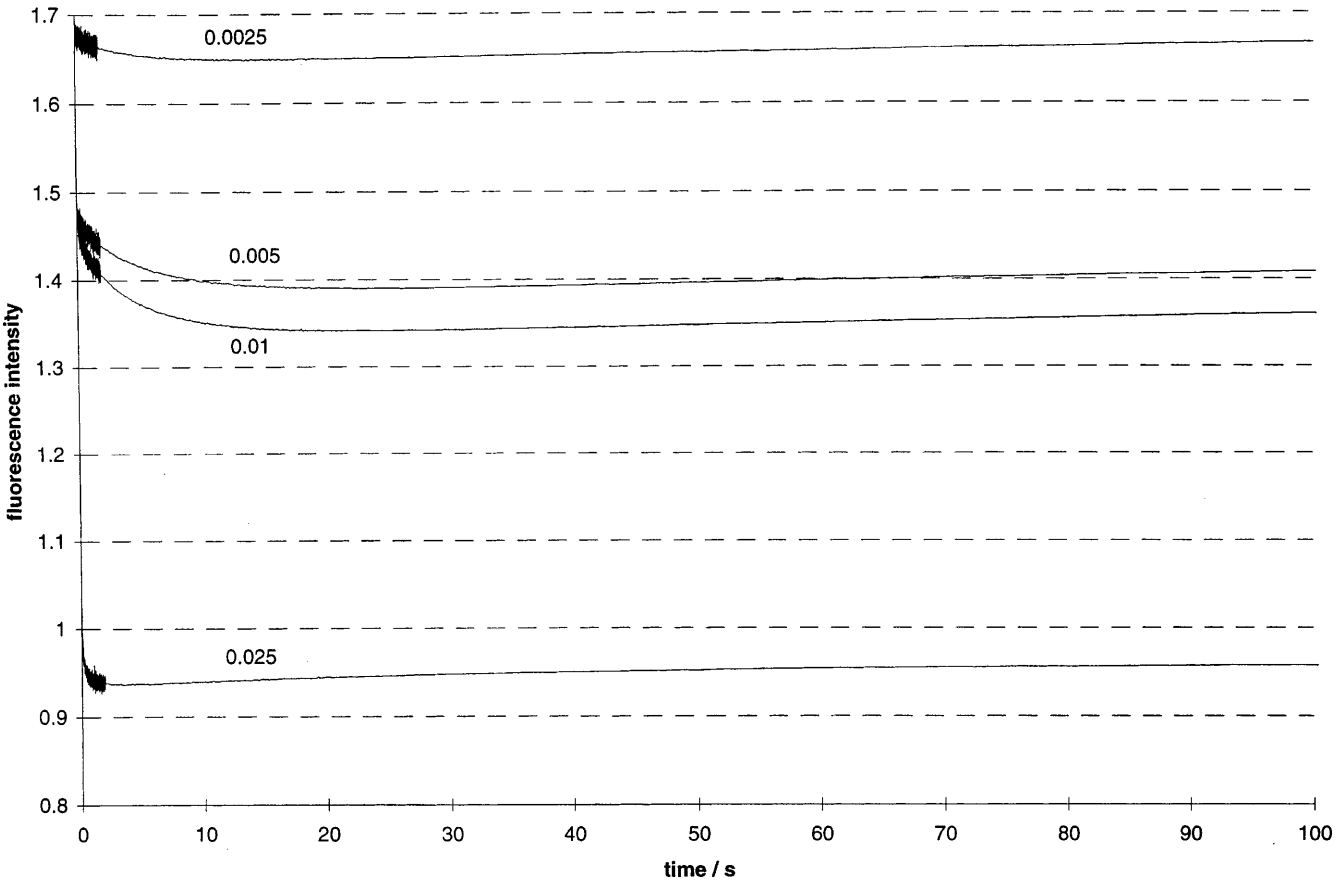

Fig. 5 The fluorescence intensity as a function of time for the mixing of TNS-CApS complexes with NSP. The final concentration was 0.01%wt CApS and the concentration of NSP is given in weight percent. All solutions contained 0.005%wt TNS and 5 mM NaCl, and the pH was 8.0. The excitation wavelength was 315 nm

electrostatic and nonelectrostatic contributions to CApS binding of TNS are at least partially coupled, and not associated with independent sites. This conclusion was already reached in Ref. [1], on the basis of independent spectroscopic results. The emission spectra showed that there is only one type of binding site for TNS on CApS, and that it had a very similar hydrophobic enviroment to that in NApS except for the presence of charges near the binding sites in CApS. The situation is very similar to that observed with DNA [7], where, for example, intercalative or groove binding modes provide both electrostatic and nonelectrostatic (hydrophobic, hydrogen bonding) interactions at the same time.

There is thus a distinct difference in the effect of simple salts (NaCl) and NSP on the binding of TNS. Increasing concentrations of salt screen the electrostatic interaction, but even at high salt a substantial amount of TNS remains bound by nonelectrostatic interactions [1]. By contrast, the anionic NSP eliminate TNS binding altogether by both competing for the electrostatic attraction on the CApS, and by preventing TNS from exploiting the nonelectrostatic forces. The simplest explanation for this additional effect of the particles is steric exclusion, where particles which are bound only electrostatically also prevent nonelectrostatic TNS binding by their mere size occupancy.

The above observations were used as a basis for recalculating the intensity data of Fig. 3a into the amount of NSP bound to CApS. The basic assumption is that the decrease in TNS fluorescence intensity is proportional to the amount of adsorbed NSP, i.e. that each particle displaces the same number of TNS molecules. Furthermore it was assumed that the remaining weak fluorescence at high concentrations of NSP was due to free TNS. This background intensity was therefore subtracted in order to correct for (the small) intensity contributions from free TNS. The resulting binding isotherm (Fig. 3b) reveals a high affinity between NSP and CApS. The linear relation at low NSP concentrations indicates stoichiometric binding. Between mass ratios m_{NSP}/m_{CApS} of 1 and 2 the linear growth is lost, and at mass ratios higher than 2 the constant amount of bound NSP shows that all available sites are occupied by NSP. The rather abrupt switch from stoichiometric binding to saturation indicates a substantial affinity constant.

The titration represented in Fig. 1 corresponds to a horizontal path in the phase diagram of Fig. 6. One important observation is that the shapes of the (normalized) TNS emission spectra (Fig. 1) do not change substantially during the titration with NSP. This indicates that TNS is bound in the same way to CApS irrespective of whether it forms white or transparent flocs. Furthermore, it indicates that TNS release can be used to measure the number of bound particles in a manner which allows comparison under different states of flocculation.

A comparison of the binding isotherm (Fig. 2b) with the phase diagram (Fig. 6) shows that the mixing weight ratio m_{NSP}/m_{CApS} of about 1 where the white flocs form (white channel-like area in Fig. 6) corresponds to the rather narrow region of the isotherm where the binding (Fig. 2b) switches from being stoichiometric to being saturated. Thus, under the condition $m_{NSP} \approx m_{CApS}$ many of the cationic sites are occupied by NSP but there are still positive sites available on the polymer. This is an ideal situation for patch flocculation, which has been the mechanism suggested for the white flocs [2]. At lower concentrations of NSP, fewer particles are bound to CApS maybe in a manner where several polymer strands in the branched parts of CApS cover the particles and render then inefficient for patch flocculation. This situation corresponds to that region of transparent floc formation (dark area) which is to the left of the channel in Fig. 6. Transparent flocs also form at mixing weight ratios well above 1 (dark area to the right in Fig. 6). According to Fig. 2b these conditions correspond to the saturated part of the isotherm, where all sites are occupied by particles, and again patch flocculation can be expected to become inefficient. Importantly, charge reversal of the complexes is not observed even at saturating concentrations of NSP, as measured by electrokinetic methods [8]. The complexes are thus still positively charged, meaning that some cationic groups do not participate in silica binding, for steric or other reasons, but still contribute to the electrophoretic mobility of the complexes. The saturating density of bound particles is 0.03%wt under present conditions (dashed lines in Fig. 2b), which corresponds to $m_{NSP}/m_{CApS} = 0.6$. In terms of molar ratio this means one silica particle per 25000 glucose monomers, or about 1000 cationic charges. In other words the saturating density is 11 particles per CApS molecule. Light-scattering data suggested the saturating density to be 100 particles per CApS molecule based on fitting the scattered intensity assuming one CApS molecule per aggregate [4]. However, this assumption is questionable since it was shown that CApS molecules aggregate slightly in the presence of salt. Assuming that the aggregates totally dominate the scattered intensity the following equation can be applied,

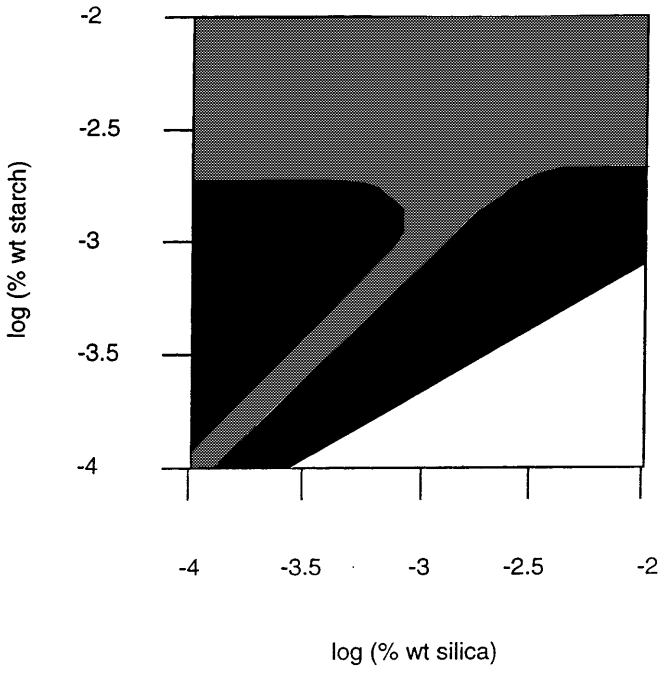

Fig. 6 Schematic phase diagram for mixtures of CApS polymer and NSP in 5 mM NaCl and at pH 8.00. In the *black areas* there are transparent flocs and in the *grey area* there are white flocs. In the *white area* there are no visible flocs. The *axes* refer to weight fraction of starch and silica, respectively, in water

$$R_{total} = N_{NSP}R_{NSP} + N_{CApS}R_{CApS} \quad , \tag{1}$$

where R is the Rayleigh ratio of the total scattered intensity of NSP and CApS, respectively, and N is the

Table 1 A recalculation of the average number of cationic amylopectin starch (*CApS*) particles and nanosized silica particles (*NSP*) in each aggregate from the scattered intensity data in Ref. [4]. The data shown in Fig. 2b are used to obtain the number of bound particles, x, to each CApS molecule. The data were recalculated according to Eq. 2

m_{NSP}/m_{CApS}	x	$R_{total}(m^{-1})$	$R_{NSP}(m^{-1})$	$R_{CApS}(m^{-1})$	N_{CApS}
0.3	6	0.497	0.0105	0.271	1.5
0.5	8	0.496	0.0107	0.271	1.4
3.5	11	1.774	0.0124	0.271	4.3
4.0	11	1.099	0.0127	0.271	2.7
5.0	11	1.547	0.0133	0.271	3.7

number of NSP and CApS per aggregate. The number of NSP bound to each CApS molecule at a given weight ratio is obtained from Fig. 2b. Consequently, Eq. (1) can be rewritten as

$$N_{\mathrm{CApS}} = R_{\mathrm{total}}/(xR_{\mathrm{NSP}} + R_{\mathrm{CApS}}) \ , \qquad (2)$$

where x is the number of NSP bound to each CApS. The results are summarized in Table 1. The results indicate that the aggregates contain between 1.5 and 4 CApS molecules. This could be expected since the mixing of NSP particles and CApS molecules is a random process. This simple calculation demonstrates the sensitivity of the result, which depends on the number of CApS molecules allowed in each aggregate. Thus the saturated density of NSP to CApS obtained from TNS release is probably the most reliable.

Kinetic measurements

Earlier we reported that two types of turbidity time curves were encountered in stopped-flow measurements of CApS-NSP interactions (Fig. 4, [2]). One type exhibits a maximum in turbidity, with an initial increase up to about 40 ms being followed by a decrease in turbidity. This type of response is observed for mixing ratios $m_{\mathrm{NSP}}/m_{\mathrm{CApS}}$ which deviate substantially from 1:1, i.e in the parts of the phase diagram where transparent flocs are formed. In the second type of response the turbidity increases monotonously. An initial fast increase lasts for about 40 ms and is followed by a slower increase in turbidity. This second type of response corresponds to a situation where white flocs are formed, i.e. at weight ratios close to 1. The turbidity measurements [2] were performed at CApS concentrations of 0.1%wt, which is a factor of 10 higher than the 0.01 %wt concentration of CApS used in the present fluorescence measurements. (Also the NSP concentrations was lower in the present experiments so similar mixing ratios were studied.) However, the fact that the channel-like area of white-flock formation (grey in Fig. 6) extends down to the polymer/particle concentrations used here indicates that the same type of flocculation behavior also occurs at the lower concentrations. The results of flocculation kinetics based on TNS emission can thus be used to interpret the turbidity-based data.

Turbidity and TNS emission can be expected to monitor different aspects of the flocculation process. As deduced earlier, TNS emission reflects the number of bound silica particles in a manner which is rather insensitive to the global state of the complex (cf. Fig. 2b). This is also supported by the observation that the affinity of TNS seems to be rather insensitive to the CApS polymer conformation (coil size) [1]. Turbidity, on the other hand, reflects the degree of inhomogeneity in the distribution of the particles, because the polymer is a comparatively poor scatterer, and will therefore be sensitive to the global state of the particle-polymer complex. Binding to CApS, also seen by TNS release, will certainly increase this inhomogeneity substantially, since the particles will accumulate in the polymer coils. In addition turbidity will also reflect changes in the polymer conformation once the particles are bound because it will change their spatial distribution. To a first degree of approximation we will assume that TNS emission only reflects the number of bound particles, whereas turbidity also includes effects of polymer conformational changes. The effects are not independent of course. A change in polymer conformation might affect not only the spatial arrangement of the particles but also how many particles are bound, which in turn will affect TNS emission. Such secondary, indirect effects are thus neglected at the present level of analysis.

The most important conclusion from the fluorescence kinetics is that a clear majority of the particles (at a certain mixing ratio) bind to CApS within a few milliseconds, since a large part of the initial TNS emission has disappeared before the first measurement point (Fig. 5a). Importantly, because the concentrations of CApS and NSP are 10 times higher, the particle binding in the turbidity studies [2] can only be faster than measured by TNS release, approximately by a factor of 100. It can therefore be concluded that particle binding is finished well before the characteristic time of 40 ms in the turbidity curves [2], where depending on mixing ratio the turbidity either takes on a slower rate of growth or starts to decrease. Thus, the first increasing part which is present in both types of turbidity curves most likely includes enhanced scattering due to the particle binding process itself and a contraction of the branched polymer coil due to screening of the cationic charges by the anionic particles. This latter effect is very important in the interaction between linear cationic polyacrylamide and NSP [9]. The second part of the response must therefore reflect a process which occurs after the polymer has been decorated with particles, and which could be changes in the conformation of individual polymers or the formation of supramolecular aggregates (transparent or white flocs).

In earlier work [2] we proposed several contributions to the turbidity curves:

1. Binding of NSP to CApS,
2. Initial screening of the cationic charges on CApS by NSP,
3. Flocculation between different amylopectin molecules decorated with NSP
4. Conformational changes in the NSP-decorated amylopectin molecule induced by electrostatic repulsion and/or hydrodynamic shearing.

The present investigation has shown (as speculated earlier [2]) that the binding contribution (1) is so fast that it is more or less complete when the turbidity measurements start. Therefore the initial screening (2) and the subsequent contraction are probably the most important factors for the initial turbidity increase. Regarding (4) it was proposed that the decrease in turbidity after the maximum in the turbidity kinetics under conditions of transparent floc formation reflects an expansion of the coil, as a result of electrostatic repulsion between adsorbed silica particles. Such an effect would reduce the polymer-induced inhomogeneity in the particle distribution, and thus lower the scattering power. Interestingly, the weak increase in TNS fluorescence we observe in this time range (Fig. 5a) could correspond to slightly enhanced TNS binding due to less electrostatic repulsion by a more diluted particle distribution.

The present results show that fluorescence techniques give valuable independent information on flocculating systems, albeit in their present design they cannot shine light on the possibility of shear-induced deformation, or provide direct information on process (3), the formation of flocs. There is potential, however. Anisotropic deformations of polymers may be monitored through fluorescence-detected linear dichroism (see Ref. [10] for a review of polarized spectroscopy), and fluorescence energy transfer is a powerful technique for studies of the formation of supramolecular aggregates [11]. Interestingly both approaches can be implemented with the stopped-flow technique.

Acknowledgements Per Lincoln and Bo Albinsson are gratefully acknowledged for useful help and ideas concerning the spectrophotometric measurements. Eka Chemicals AB is gratefully acknowledged for financial support.

Appendix

An estimate of the concentration of CApS-bound TNS was obtained from Eq. 3 of Ref. [1] by assuming a site TNS size of one glucose monomer.

$$[\mathrm{TNS}]_{\mathrm{bound}} = \frac{[\mathrm{glucose}]_{\mathrm{tot}} + [\mathrm{TNS}]_{\mathrm{tot}} + K_{\mathrm{d}}}{2} - \sqrt{\frac{([\mathrm{glucose}]_{\mathrm{tot}} + [\mathrm{TNS}]_{\mathrm{tot}} + K_{\mathrm{d}})^2}{4} - [\mathrm{TNS}]_{\mathrm{tot}}[\mathrm{glucose}]_{\mathrm{tot}}} \; .$$

With $K_{\mathrm{d}} = 9$ mM (at 5 mM NaCl) and total concentrations of TNS and glucose monomers of 14.6 μM and 61.7 μM, respectively, we obtain $[\mathrm{TNS}]_{\mathrm{bound}} = 9.92 \times 10^{-8}$ M, which gives a binding ratio $\frac{[\mathrm{TNS}]_{\mathrm{bound}}}{[\mathrm{glucose}]_{\mathrm{tot}}} = 1.61 \times 10^{-3}$.

References

1. Dahlberg A, Larsson A, Åkerman B, Wall S (1998) Colloid Polym Sci 277:428–435
2. Larsson A, Wall S (1999) Colloids Surf A 139:259
3. Larsson A (1999) Colloid Polym Sci (in press)
4. Larsson A (1998) Colloids Surf B 12:23
5. Biddle D, Walldal C, Wall S (1996) Colloids Surf A 118:89
6. Iler RK (1979) In: The chemistry of silica. Wiley, New York, pp 187–189
7. Bloomfield VA, Crothers DM, Tinoco I (1974) In: Physical chemistry of nucleic acids. Harper & Row, New York, pp 429–431
8. Larsson A, Rasmusson M (1997) Carbohydr Res 304:315
9. Walldal C, Wall S, Biddle D (1998) Colloids Surf A 131:203
10. Norden B, Kubista M, Kurusev T (1992) Q Rev Biophys 25:51
11. Stryer L (1978) Annu Rev Biochem 47:819